PHYSICAL REVIEW A **75**, 042506 (2007)

Excited states of positronic atoms

M. W. J. Bromley*
Department of Physics and Computational Sciences Research Center, San Diego State University, San Diego, California 92182, USA

J. Mitroy†
Faculty of Technology, Charles Darwin University, Darwin NT 0909, Australia

(Received 5 January 2007; published 19 April 2007)

The existence and structure of positronic atoms with a total angular momentum of $L=1$ is studied with the configuration interaction method. Evidence is presented that there is a $^2P^o$ state of e^+Ca and $^{2,4}P^o$ states of e^+Be($^3P^o$) that are electronically stable with binding energies of 45 meV and 2.6 meV, respectively. These predictions rely on the use of an asymptotic series analysis to estimate the angular $L\rightarrow\infty$ limit of the energy. Incorporating corrections that compensate for the finite range of the radial basis increased the binding energies of e^+Ca and e^+Be to 71 meV and 42 meV, respectively.

DOI: 10.1103/PhysRevA.75.042506 PACS number(s): 36.10.Dr, 34.85.+x, 71.60.+z

I. INTRODUCTION

The existence of positron-atom bound states is now firmly established and about ten atoms have been identified as being able to bind a positron [1]. Beside their intrinsic interest, the knowledge that positrons can form bound states has been crucial to recent developments in understanding the very large annihilation rates that occur when positrons annihilate with various molecules in the gas phase [2–9]. One common feature of the atomic calculations is that binding only occurs to atoms with an ionization energy close to 6.80 eV (the Ps binding energy) and the binding energies are largest for those atoms with ionization energies closest to 6.80 eV [1].

The existence of positronic bound states with nonzero angular momentum was an open question until the recent identification of the $^2P^o$ state of e^+Ca as electronically stable [10]. There are two types of excited state that can be considered. In one case, the positron is bound to an excited state of the parent atom. An example of such a state (with zero orbital angular momentum) is the metastable e^+He($^3S^e$) state [11]. The other type of state could be regarded as a positron, in an excited orbital, bound to the ground state of the parent atom. The recently discovered $^2P^o$ state e^+Ca can be regarded as such a state since it has the same dissociation channel as the lower lying $^2S^e$ e^+Ca ground state [10].

The present article describes some very large configuration interaction (CI) calculations of the $^2P^o$ states of e^+Ca and e^+Sr that indicate the presence of a $^2P^o$ bound state for e^+Ca with a binding energy of 45 meV. The situation for e^+Sr is less clear and the best that can be said is that there may be a $^2P^o$ state that is just bound with a binding energy of 5 meV or smaller. Since the ionization energies of the Ca and Sr atoms are less than 6.80 eV, the thresholds for a stable positron complex are those of the $[\mathrm{Ca}^+(4s),\mathrm{Sr}^+(5s)]$ +Ps($1s$) dissociation channels.

The other state that is investigated is the $^{2,4}P^o$ state of e^+Be with the metastable Be $2s2p^3P^o$ state being the dominant configuration of the parent atom. The resulting e^+Be state is stable with a binding energy of at least 2.6 meV with respect to the $\mathrm{Be}^+(2p)$+Ps($1s$) dissociation channel.

II. DESCRIPTION OF THE CALCULATIONS

A. The model Hamiltonian

The CI method as applied to positron-atomic systems with two valence electrons and a positron has been discussed previously [12–14], but a short description is worthwhile. The model Hamiltonian is initially based on a Hartree-Fock (HF) wave function for the neutral-atom ground state. One- and two-body semiempirical polarization potentials are added to the potential field of the HF core and the parameters of the core-polarization potentials defined by reference to the spectrum of the singly ionized parent atom [12,13].

All calculations were done in the frozen-core approximation. The effective Hamiltonian for the system with two valence electrons and a positron was

$$H = -\frac{1}{2}\nabla_0^2 - \sum_{i=1}^{2}\frac{1}{2}\nabla_i^2 - V_{\mathrm{dir}}(\mathbf{r}_0) + V_{\mathrm{p1}}(\mathbf{r}_0) + \sum_{i=1}^{2}[V_{\mathrm{dir}}(\mathbf{r}_i) + V_{\mathrm{exc}}(\mathbf{r}_i) + V_{\mathrm{p1}}(\mathbf{r}_i)] - \sum_{i=1}^{2}\frac{1}{r_{i0}} + \sum_{i<j}^{2}\frac{1}{r_{ij}} - \sum_{i<j}^{2}V_{\mathrm{p2}}(\mathbf{r}_i,\mathbf{r}_j) + \sum_{i=1}^{2}V_{\mathrm{p2}}(\mathbf{r}_i,\mathbf{r}_0). \quad (1)$$

The potential, V_{dir}, represents the direct part of the interaction with the HF electron core. It is attractive for electrons and repulsive for the positron. The exchange potential (V_{exc}) between the valence electrons and the HF core was computed without approximation.

The one-body polarization potentials (V_{p1}) are semiempirical in nature and are derived from an analysis of the singly ionized parent atoms. They have the functional form

*Electronic address: mbromley@physics.sdsu.edu
†Electronic address: jxm107@rsphysse.anu.edu.au

$$V_{\mathrm{p1}}(r) = -\sum_{\ell m} \frac{\alpha_d g_\ell^2(r)}{2r^4} |\,\ell\, m\rangle\langle \ell\, m|. \tag{2}$$

The factor α_d is the static dipole polarizability of the core and $g_\ell^2(r)$ is a cutoff function designed to make the polarization potential finite at the origin. The same cutoff function has been adopted for both the positron and electrons due to lack of information that can be used to tune the positron cutoff. This will tend to lead to an underestimation of the strength of the positron polarization potential since the electron-atom polarization potential is weaker than the positron-atom polarization potential for closed shell targets [1,15,16]. The error should be small since the core polarizabilities for all the systems studied are at least 30 times smaller than the valence polarizabilities. In this work, $g_\ell^2(r)$ was defined to be

$$g_\ell^2(r) = 1 - \exp(-r^6/\rho_\ell^6), \tag{3}$$

where ρ_ℓ is an adjustable parameter. The two-body polarization potential (V_{p2}) is defined as

$$V_{\mathrm{p2}}(\mathbf{r}_i,\mathbf{r}_j) = \frac{\alpha_d}{r_i^3 r_j^3}(\mathbf{r}_i \cdot \mathbf{r}_j) g_{\mathrm{p2}}(r_i) g_{\mathrm{p2}}(r_j), \tag{4}$$

where $g_{\mathrm{p2}}(r)$ is chosen to have a cutoff parameter obtained by averaging the ρ_ℓ. The core dipole polarizabilities and the ρ_ℓ were set to the values in Refs. [12,13]. This model has been used to describe many of the features of neutral Be, Ca, and Sr to quite high accuracy [12,13,17]. All energies reported here are given relative to the energy of each doubly ionized core.

B. The trial wave function

The trial wave function adopted for the variational calculations consists of a linear combination of states which are antisymmetric in the interchange of the two electrons,

$$|\Psi; LS\rangle_a = \sum_i c_i |\Phi_i; LS\rangle_{\mathcal{A}}. \tag{5}$$

Each antisymmetrized state is constructed as a linear combination of coupled states. Two electrons (particles 1 and 2) are coupled first to each other, then the positron (particle 0) is coupled to form a state with total angular and spin angular momentum, L and S,

$$\begin{aligned}|\Phi_i; [a_1 b_2] L_I S_I p_0 LS\rangle = & \sum_{\substack{m_a,m_b,m_p,M_{L_I} \\ \mu_a,\mu_b,\mu_p,M_{S_I}}} \langle \ell_a m_a \ell_b m_b | L_I M_{L_I}\rangle \\ & \times \langle L_I M_{L_I} \ell_p m_p | L M_L\rangle \\ & \times \langle S_I M_{S_I} \tfrac{1}{2} \mu_p | S M_S\rangle |a_1 \ell_a m_a \mu_a\rangle \\ & \times |b_2 \ell_b m_b \mu_b\rangle |p_0 \ell_p m_p \mu_p\rangle. \end{aligned} \tag{6}$$

The subscript by each orbital denotes the electron occupying that particular orbital. The antisymmetric states are written as

$$\begin{aligned}|\Phi_i; [ab] L_I S_I p LS\rangle_{\mathcal{A}} = & \frac{1}{\sqrt{2(1+\delta_{ab})}} (|[a_1 b_2] L_I S_I p_0\rangle \\ & + (-1)^{l_a + l_b + L_I + S_I} |[a_2 b_1] L_I S_I p_0\rangle). \end{aligned} \tag{7}$$

The CI basis was constructed by letting the two electrons and the positron form all the possible total angular momentum $L_T = 1$ configurations, with the two electrons in a spin-singlet state (for Ca and Sr), subject to the selection rules,

$$\max(\ell_0, \ell_1, \ell_2) \le J, \tag{8}$$

$$\min(\ell_1, \ell_2) \le L_{\mathrm{int}}, \tag{9}$$

$$(-1)^{(\ell_0 + \ell_1 + \ell_2)} = -1. \tag{10}$$

In these rules ℓ_0, ℓ_1, and ℓ_2 are respectively the orbital angular momenta of the positron and the two electrons. We define $\langle E\rangle_J$ to be the energy of the calculation with a maximum orbital angular momentum of J.

The main technical problem afflicting CI calculations of positron-atom interactions is the slow convergence of the energy with J [1,14,18,19]. One way to determine the $J \to \infty$ energy, $\langle E\rangle_\infty$, is to make use of an asymptotic analysis. It has been shown that successive increments, $\Delta E_J = \langle E\rangle_J - \langle E\rangle_{J-1}$, to the energy can be written as an inverse power series [14,20–23], viz.,

$$\Delta E_J \approx \frac{A_E}{\left(J+\frac{1}{2}\right)^4} + \frac{B_E}{\left(J+\frac{1}{2}\right)^5} + \frac{C_E}{\left(J+\frac{1}{2}\right)^6} + \cdots. \tag{11}$$

The $J \to \infty$ limit has been determined by fitting sets of $\langle E\rangle_J$ values to asymptotic series with either 1, 2, or 3 terms. The linear factors, A_E, B_E, and C_E for the three-term expansion are determined at a particular J from four successive energies ($\langle E\rangle_{J-3}$, $\langle E\rangle_{J-2}$, $\langle E\rangle_{J-1}$, and $\langle E\rangle_J$). Once the linear factors have been determined it is trivial to sum the series to ∞ and thus obtain the variational limit. Application of asymptotic series analysis to helium has resulted in CI calculations reproducing the ground-state energy to an accuracy of $\sim 10^{-8}$ hartree [23,24].

III. THE $^2P^o$ STATE OF e^+Ca

The ionization potential of Ca is 0.2247 hartree [25], so the condition for stability of a e^+Ca state is that its energy be less than that of the $Ca^+(4s)+Ps(1s)$ threshold. The threshold for binding is −0.686 286 53 hartree since the energy of the $Ca^+(4s)$ state is −0.436 286 53 hartree in the present model potential (relative to the energy of the doubly ionized Ca^{2+} core).

The Hamiltonian for the e^+Ca $^2P^o$ state was diagonalized in a CI basis constructed from a very large number of single particle orbitals, including orbitals up to $\ell = 14$. The two electrons were in a spin singlet state. There was a minimum of 14 radial basis functions for each ℓ. The largest calculation was performed with $J = 14$, $L_{\mathrm{int}} = 3$, and the CI basis had a dimension of 874 888. The parameter L_{int} does not have to be

TABLE I. Results of CI calculations for the e^+Ca $^2P^o$ state as a function of J, and for $L_{\rm int}=3$. The total number of configurations is denoted by N_{CI} while the number of electron and positron orbitals are denoted by N_e and N_p. The three-body energy of the state, relative to the energy of the Ca^{2+} core, is given in hartree. The threshold for binding is −0.686 286 53 hartree, and $\langle\varepsilon\rangle_J$ gives the binding energy against dissociation into Ps+$Ca^+(4s)$. The mean electron-nucleus distance $\langle r_e\rangle$ and the mean positron-nucleus distance $\langle r_p\rangle$ are given in units of a_0. The $\langle\Gamma_v\rangle$ and $\langle\Gamma_c\rangle$ columns give the valence and core annihilation rates, respectively (in units of 10^9 s^{-1}). The entries in the row labeled 14^* were computed with $L_{\rm int}=2$. The extrapolated results used Eq. (11) to estimate the $J\to\infty$ corrections. The largest values of $\langle X\rangle_J$ were used in the extrapolations.

J	N_e	N_p	N_{CI}	$\langle E\rangle_J$	$\langle\varepsilon\rangle_J$	$\langle r_e\rangle$	$\langle r_p\rangle$	$\langle\Gamma_c\rangle$	$\langle\Gamma_v\rangle$
10	158	154	576184	−0.67981518	−0.00647135	4.70225	7.62604	0.0062905	0.655314
11	172	168	650860	−0.68106444	−0.00522209	4.74800	7.63988	0.0061615	0.705043
12	186	182	725536	−0.68207134	−0.00421520	4.78940	7.66182	0.0060370	0.749092
13	200	196	800212	−0.68289035	−0.00339618	4.82683	7.68815	0.0059205	0.788275
14	214	210	874888	−0.68356185	−0.00272468	4.86006	7.71578	0.0058158	0.823311
14^*	214	210	556192	−0.68313606	−0.00315047	4.86933	7.74778	0.0056885	0.816812
				$J\to\infty$ extrapolations					
one-term Eq. (11)				−0.68648706	0.0002005	5.00481	7.83614	0.005359	1.31422
two-term Eq. (11)				−0.68739784	0.0011113	5.08759	7.96357	0.005079	1.41897
three-term Eq. (11)				−0.68763826	0.0013517	5.11457	8.02355	0.005021	1.42395

large since it is mainly concerned with electron-electron correlations [13]. The resulting Hamiltonian matrix was diagonalized with the Davidson algorithm [26], and a total of 10 000 iterations were required for some of the most slowly convergent cases.

The energy and other expectation values of the e^+Ca $^2P^o$ state as a function of J is given in Table I. The binding energy is defined as $\langle\varepsilon\rangle_J=-\langle E\rangle_J-0.686\,286\,53$. None of the explicit calculations listed in Table I formally bind the positron.

Figure 1 shows the running estimates of $\langle E\rangle_\infty$ with the $J\to\infty$ extrapolations as a function of J. The two-term and three-term extrapolations both give energies below the dissociation threshold and indicate that the e^+Ca $^2P^o$ state is electronically stable. The three-term extrapolation seems to have stabilized at a binding energy of ≈0.001 35 hartree. The two-term binding energy is slightly smaller but does seem to be approaching the three-term estimate. The one-term estimate of $\langle E\rangle_\infty$ is also absolutely bound, although its binding energy is somewhat smaller. The precise estimates of $\langle E\rangle_\infty$ evaluated at $J=14$ for the different extrapolations are given in Table I.

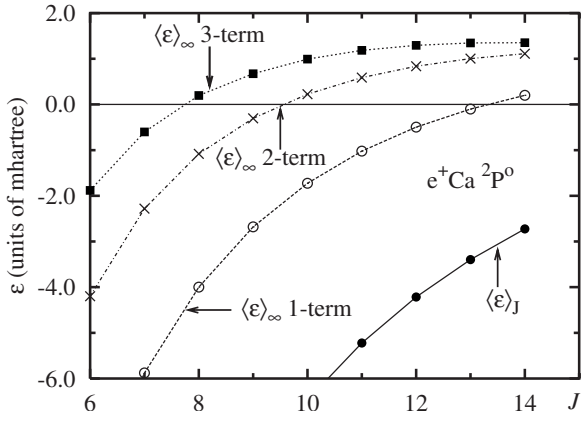

FIG. 1. The binding energy (units of hartree) of the $^2P^o$ state of e^+Ca as a function of J. The directly calculated energy is shown as the solid line while the $J\to\infty$ limits using Eq. (11) with one, two, or three terms are shown as the dashed lines. The $Ca^+(4s)$+Ps$(1s)$ dissociation threshold is shown as the horizontal solid line.

With a very small binding energy it is desirable to look at the areas of uncertainty in the model and computation to determine whether they could invalidate the prediction of binding. The impact of variations in the core polarization potentials have been discussed previously [10], and are unlikely to invalidate the prediction of the bound state.

The lack of completeness in the finite dimension radial basis is also not an issue since this is expected to lead to the binding energy being underestimated. Previous CI investigations have revealed that accurate prediction of the ΔE_J energy increments required a larger basis as J increases [14,23]. This results in the typical CI partial wave expansion, with a fixed dimension radial basis for the different L values, having an inherent tendency to underestimate the binding energy [14,23]. There will be more discussion about this point later.

The choice of $L_{\rm int}=3$ leads to some underestimation in the binding energy. Table I gives the energy for the $J=14$, $L_{\rm int}=2$ calculation. A one-term form of Eq. (11) is used to extrapolate the $J=14$ energy to the $L_{\rm int}\to\infty$ limit. The resultant e^+Ca energy was $E=-0.683\,884\,76$ hartree, a decrease of 0.000 32 hartree. Adding this to the three-term $\langle E\rangle_\infty$ energy would result in a total binding energy of $\langle\varepsilon\rangle=0.001\,67$ hartree, an increase of about 24%. This energy can be regarded as giving a better estimate than 0.001 35 hartree.

The spin-averaged valence annihilation rate is the most important of the other expectation values listed in Table I. The convergence in J is even worse than the energy since the successive increments to Γ scale as $1/J^2$ as J increases. The extrapolation to the $J\to\infty$ limits were done using a series almost the same as Eq. (11), but with the first term starting as

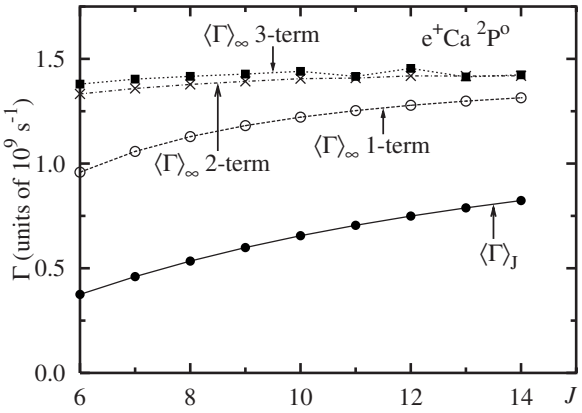

FIG. 2. The annihilation rate (in units of 10^9 s^{-1}) of the $^2P^o$ state of e^+Ca as a function of J. The directly calculated annihilation rate is shown as the solid line while the $J\to\infty$ limits using Eq. (11) with one, two, or three terms are shown as the dashed lines.

$A_\Gamma/(J+1/2)^2$. The running estimates of $\langle\Gamma\rangle_\infty$ are shown in Fig. 2. The estimate using three-terms in Eq. (11) should be the best. However, the three-term curve in Fig. 2 shows fluctuations for $J>10$ that are caused by the imprecision in the eigenvector obtained from the Davidson algorithm. Similar fluctuations (although smaller in magnitude) were present in an investigation of the convergence of the electron-electron δ function for the helium ground state [23].

The trends shown in Fig. 2 indicate that a converged calculation would give an annihilation rate of $\Gamma\approx 1.5\times 10^9$ s^{-1}. The large value of the annihilation rate suggests that a large fraction of the wave function consists of the positron attached to the electron in a Ps($1s$) cluster.

Table I also gives other expectations such as the mean positron and electronic distances, and the core annihilation rate. The $J\to\infty$ limits are once again computed using an asymptotic series. The leading term of the asymptotic series for these other operators have not yet been established by perturbation theory, but a leading-order term of $A/(J+1/2)^4$ is assumed to be valid in the present analysis. For the most part the $J\to\infty$ corrections lead to 5% changes in the expectation values.

The mean positron radius, $\langle r_p\rangle$ is estimated to be about $8.0a_0$. The system is compact despite its small binding energy (the e^+Ca $^2S^e$ ground state with a binding energy ten times larger has $\langle r_p\rangle\approx 6.9a_0$ [27]). The large r form of the wave function must have a $Ca^+(4s)+Ps(1s)$ structure with the Ps($1s$) center of mass being in an $L=1$ state with respect to the residual ion. The centrifugal barrier associated with the nonzero angular momentum acts to confine the positron probability distribution.

The electron and positron probability densities are depicted in Fig. 3. As expected, the peak of positron density is outside the electron density peak. One expects the electron and positron densities to approach each other as $r\to\infty$ since the lowest energy breakup is into the Ca^++Ps($1s$) channel. However, the positron density is significantly larger than the electron density at $r=12a_0$. This indicates a considerable degree of polarization in the Ps cluster which seems to be orientated with the electron closest to the nucleus.

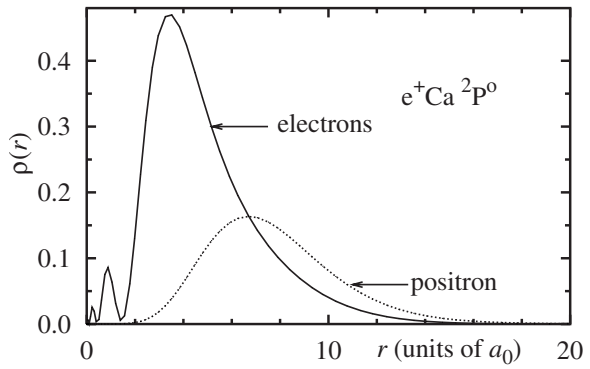

FIG. 3. Electron and positron probability densities ($\rho(r)$) as a function of r. The electron density is normalized to 2 while the positron density is normalized to 1.

IV. THE $^2P^o$ STATE OF e^+Sr

Since the ionization potential of strontium is 0.2093 hartree [28], the lowest-energy dissociation channel is that of $Sr^+(5s)+Ps(1s)$. The calculations carried out on the e^+Sr $^2P^o$ state (with the two electrons in a spin singlet state) were very similar to those discussed for e^+Ca. The only difference in the dimensionality was that there was an additional $\ell=2$ electron orbital. Even the exponents of the Laguerre orbitals were almost identical.

The energies for the sequence of calculations are given in Table II. The current sequence of calculation does not result in binding even when the $J\to\infty$ extrapolation are included. Figure 4 shows the running estimates of $\langle\varepsilon\rangle_\infty$ as a function of J. The three-term extrapolation asymptotes to an energy that is 0.001 77 hartree away from binding. The system still remains unbound when the $L_{\rm int}\to\infty$ correction of 0.000 37 hartree is added to the energy.

An unbound system would be expected to have an $\langle\varepsilon\rangle_\infty$ that asymptotes to zero. The present calculation does not asymptote to zero, and this indicates that the basis is not

TABLE II. Results of CI calculations for the $^2P^o$ state of e^+Sr for a series of J, with fixed $L_{\rm int}=3$. The threshold for binding is −0.655 349 76 hartree, and $\langle\varepsilon\rangle_J$ gives the binding energy against dissociation into Ps+$Sr^+(5s)$. Other aspects of the table are similar to those of Table I.

J	N_e	N_p	N_{CI}	$\langle E\rangle_J$	$\langle\varepsilon\rangle_J$
10	159	154	590590	−0.64373343	−0.01161633
11	173	168	666834	−0.64528075	−0.01006902
12	187	182	743078	−0.64653069	−0.00881908
13	201	196	819322	−0.64755027	−0.00779949
14	215	210	895566	−0.64838906	−0.00696071
14*	215	210	576870	−0.64790288	−0.00744688
			$J\to\infty$ extrapolations		
one-term Eq. (11)				−0.65204302	−0.0033067
two-term Eq. (11)				−0.65322302	−0.0021267
three-term Eq. (11)				−0.65356839	−0.0017714

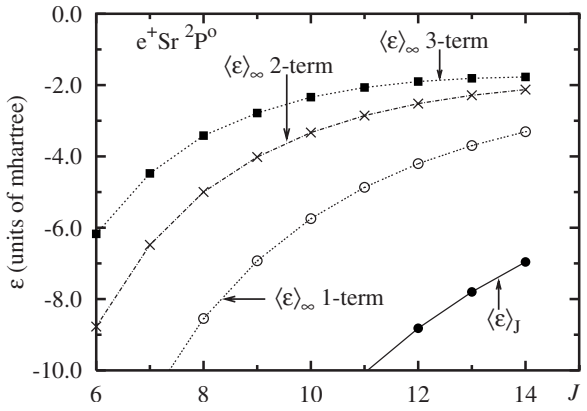

FIG. 4. The binding energy of the e^+Sr system as a function of J. The directly calculated energy is shown as the solid line while the $\langle\varepsilon\rangle_\infty$ limits using Eq. (11) are shown as the dashed lines. The $Sr^+(5s)+Ps(1s)$ dissociation threshold is at $\langle\varepsilon\rangle=0$.

large enough to properly represent the $Sr^+ + Ps(1s)$ dissociation channel at $\varepsilon=0$. Usage of a finite dimension, and consequently a finite-range basis results in the diagonalization of the Hamiltonian in a soft sided box. The question of whether enlargement of the radial basis would result in a bound state is addressed later.

V. POSITRON BINDING TO THE Be $^3P^o$ STATE

The ionization potential of the Be($^3P^o$) state is 6.598 eV and, therefore, it had been earlier identified as a state that could possible bind a positron [1,29,30]. The $2s2p\ ^3P^o$ states are metastable with the $^3P_2^o$ and $^3P_0^o$ states having lifetimes exceeding an hour [31,32]. Recently, a large CI calculation (334 248 configurations) attempted to determine whether a positron could be bound to the Be($^3P^o$) state [29]. The results of this calculation are best described as inconclusive. There are two different spin states of the positronic complex, namely $^2P^o$ and $^4P^o$, due to the triplet nature of the two electron parent, and the annihilation rates reported in Table III are spin averaged.

In the present calculation the dimension of the radial basis has been increased to 14 Laguerre-type orbitals (LTOs) per ℓ and the results of the CI calculations are tabulated in Table III as a function of J. Once again, none of the explicit CI calculations give an energy that is below the $Be^+(2s)+Ps(1s)$ threshold. The largest calculation gave an energy that was 0.001 62 hartree away from threshold.

A demonstration of binding is again reliant on the asymptotic analysis. Figure 5 shows the running estimates of $\langle\varepsilon\rangle_\infty$ as a function of J. Only the three-term extrapolation gives evidence of binding, and even here binding is not achieved until $J=12$. The final three-term estimate of the binding energy is only 8.64×10^{-5} hartree, i.e., 2.4 meV.

System limitations prevented us from performing a larger calculation, and thus establishing more firmly the stability of e^+Be($^3P^o$). It is worth noting that the inclusion of the two extra LTOs per ℓ (from the calculation in [29]) was responsible for increasing $\langle\epsilon\rangle_\infty$ at $J=12$ by 0.000 151 hartree.

The difference between the $L_{\rm int}=2$ and $L_{\rm int}=3$ energies is very small, 2.76×10^{-5} hartree. The two electrons are in a triplet state and the energy is known to converge as $A_E/(J+1/2)^6$ for such configurations [33]. The $L_{\rm int}\to\infty$ energy correction was 9.1×10^{-6} hartree. When this was added to $\langle\varepsilon\rangle_\infty$ the resultant binding energy was increased to 9.55×10^{-5} hartree, i.e., 2.6 meV.

Even though the binding energy is very small, the reliability of the prediction is high since the underlying model potential is very accurate. The main area of uncertainty in the model potential lies in the definition of the core-polarization potential. However, the Be^{2+} core polarizability of $0.0523a_0^3$ [12,17] is very small and therefore variations in the polarization potential will not have much of an impact on the energies. The polarization potential used in the present work is capable of reproducing the neutral Be static dipole and quadrupole polarizabilities to an accuracy of 0.1% [17].

The $\langle r_p\rangle_\infty$ and $\langle\Gamma_c\rangle_\infty$ estimates are not that reliable. The typical behavior of $\langle r_p\rangle_J$ for systems with an $A+Ps$ dissociation limit (where A is a single electron atom or positive ion) is for $\langle r_p\rangle_J$ to initially decrease as J increases from 1, and then to start increasing again at some higher J value (this behavior is seen in the $^2S^e$ states of e^+Ca, PsH, CuPs, and e^+Sr [12,27,34]). Since $\langle r_p\rangle_J$ is still decreasing at $J=14$ it seems probable that $\langle r_p\rangle_J$ is not yet in the asymptotic region. The core annihilation is determined by the radial distribution of the positron, and this affects the reliability of $\langle\Gamma_c\rangle_\infty$.

VI. ZERO-POINT ENERGY CORRECTIONS

Since the basis being used is of finite dimension, it also has a finite range. Consequently, the diagonalization of the Hamiltonian is performed in what is effectively a soft-sided box which will have a zero-point energy (ZPE). It is necessary to determine this ZPE in order to obtain better estimates of the binding energies, and in the case of e^+Sr, determine whether the system is bound or not. We note that Dzuba *et al.* [19,35] examined the application of ZPE energy corrections to e^+Cu and e^+Ag.

The ideas used here are based in effective range theory and quantum defect theory [36–38]. Essentially, the impact of the interactions that lead to binding on the large r form of the wave function can be represented by a couple of short-range parameters. Once these parameters have been determined, it is a simple matter to extend the range of the wave function to ∞.

The first step in the procedure was to determine the effective range of the asymptotic part of the CI basis. This is done by an initial CI calculation of the electron and positron basis sets. The complete single particle orbital basis, as used for the three-particle CI calculation, is used to form a two-particle electron-positron basis coupled to have $L=1$. The basis is diagonalized for the free positronium Hamiltonian

$$H_{\rm Ps}=-\frac{1}{2}\nabla_0^2-\frac{1}{2}\nabla_1^2-\frac{1}{r_{01}}. \tag{12}$$

The resulting energy, which is computed using an asymptotic analysis to obtain the $J\to\infty$ limit, is termed E_0.

TABLE III. Results of CI calculations for e^+Be($^3P^o$) for a series of J, with fixed $L_{\rm int}=3$. The three-body energy of the e^+-Be($^3P^o$) system, relative to the energy of the Be^{2+} core, is denoted by $\langle E\rangle_J$ (in hartree). The threshold for binding is −0.919 208 15 hartree, and $\langle\varepsilon\rangle_J$ gives the binding energy against dissociation into Ps+$Be^+(2s)$. Other aspects of the table design identical to Table I.

J	N_e	N_p	N_{CI}	$\langle E\rangle_J$	$\langle\varepsilon\rangle_J$	$\langle r_e\rangle$	$\langle r_p\rangle$	Γ_c	Γ_v
10	155	154	546252	−0.91631571	−0.00289245	3.04262	9.48204	0.0011911	0.294592
11	169	168	617988	−0.91671760	−0.00249055	3.08253	9.30895	0.0011977	0.324838
12	183	182	689724	−0.91705780	−0.00215035	3.11971	9.18345	0.0011985	0.352413
13	197	196	761460	−0.91734642	−0.00186174	3.15408	9.09058	0.0011960	0.377551
14	211	210	833196	−0.91759179	−0.00161636	3.18556	9.02154	0.0011915	0.400439
14*	211	210	515284	−0.91756437	−0.00164378	3.18605	9.02290	0.0011903	0.400400
				$J\rightarrow\infty$ extrapolations					
one-term Eq. (11)				−0.91866071	−0.0005474	3.32270	8.72078	0.001172	0.72114
two-term Eq. (11)				−0.91912365	−0.0000850	3.41455	8.73278	0.001130	0.82847
three-term Eq. (11)				−0.91928460	0.0000865	3.46732	8.78791	0.001103	0.81860

The next step involved treating Ps as a point particle with mass $M=2m_e$. The $L=1$ Hamiltonian for the free Ps center of mass,

$$H=-\frac{1}{2M}\nabla_M^2, \tag{13}$$

was diagonalized in a hard-walled finite-sized cavity of radius R to give $E_{\rm box}$. The box radius $R_{\rm box}$ was then tuned until $E_{\rm box}=E_0+0.250$.

The third step involved using a Hamiltonian with a semiempirical model potential to represent the interaction of Ps in an $L=1$ state with the atomic ion. This Hamiltonian was defined as

$$H_{\rm mp}=-\frac{1}{2M}\nabla_M^2-\frac{36R^2}{2(R^6+6^6)}-\frac{V_0}{1+\exp(2r-14)}. \tag{14}$$

This potential has the correct long-range interaction between positronium and a charged particle since the polarizability of the Ps ground state is $36a_0^3$. The energy expectation of this Hamiltonian is denoted $E_{\rm mp}$ and the wave function $\Psi_{\rm mp}$. The strength of the short-range part of the interaction, V_0 was tuned until the energy shift of the semiempirical Hamiltonian, i.e., $E_1-E_{\rm box}$, was the same as $\varepsilon_{CI}-E_0$, where ε_{CI} is the binding energy of the three-body positronic atom.

The rather complicated form of Eq. (14) was adopted to ensure the radial expectation of the model potential wave function $\langle\Psi_{\rm mp}|R|\Psi_{\rm mp}\rangle=R_{\rm mp}$ was roughly compatible with that of the three-body CI wave function. Calculations with simpler forms of Eq. (14) (i.e., there was no short-range term and the cutoff parameter in the polarization potential was tuned to the energy) gave $R_{\rm mp}\approx 6\,a_0$ which was very small for such a weakly bound Ps complex. The Ps radial expectation values for the CI wave function was taken as

$$R_{\rm Ps}=\frac{1}{2}\langle r_p\rangle+\frac{1}{2}(2\langle r_e\rangle-\langle r_{\rm ion}\rangle), \tag{15}$$

where $\langle r_{\rm ion}\rangle$ is the mean electron radius of the one electron ion that binds the Ps, e.g., $Ca^+(4s)$. The data in Tables I–III gave $R_{\rm Ps}\approx 9\,a_0$.

Once each model potential was constructed, it was a simple matter to determine the energy as $R\rightarrow\infty$. The results of these calculations upon e^+Ca, e^+Sr, and e^+Be are summarized in Table IV. The binding energy of the e^+Ca $^2P^o$ state is now 0.002 60 hartree, i.e., 71 meV. The very small binding energy of the e^+Be $^2P^o$ state has increased to 0.001 75 hartree, i.e., 42 meV. The ZPE correction is largest for e^+Be since this is the orbital basis with the smallest radial extension. The e^+Sr $^2P^o$ state becomes bound, with a binding energy of 0.000 20 hartree (5.4 meV) once the ZPE analysis is performed.

The uncertainties associated with this process are of the order of 40%. Numerical experimentation with other forms of the short-range potentials gave significant variations in the final energy. The quoted uncertainty is a reflection of those variations. States with a small $R_{\rm mp}$ tend to give a smaller ZPE energy correction than states with a larger $R_{\rm mp}$. The

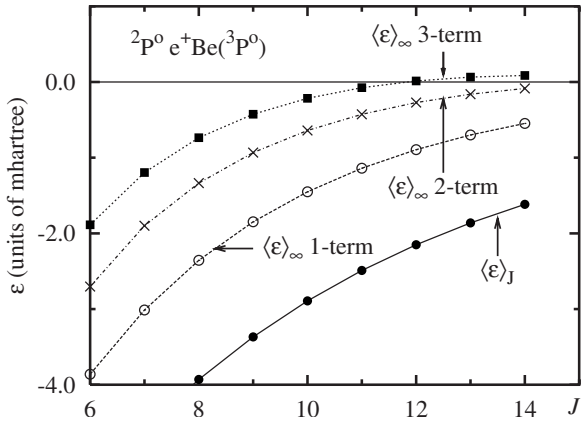

FIG. 5. The binding energy (in hartree) of the $^2P^o$ state of e^+Be as a function of J. The directly calculated energy is shown as the solid line while the $J\rightarrow\infty$ limits are shown as dashed lines. The $Be^+(2s)$+Ps($1s$) dissociation threshold is shown as the horizontal solid line.

TABLE IV. The key parameters for the zero-point energy correction analysis described in the text. The entry in the $\varepsilon_{R\to\infty}$ row gives the final energy with the ZPE energy correction. The uncertainty in $\varepsilon_{R\to\infty}$ assumes a ±40% uncertainty in the ZPE correction.

Parameter	e^+Ca	e^+Sr	e^+Be
$E_0+0.250$	0.0184	0.0180	0.0204
ε_{CI}	1.67×10^{-3}	-1.40×10^{-3}	9.55×10^{-5}
R_{box}	16.54	16.75	15.74
V_0	0.04843	0.04284	0.04607
$\varepsilon_{R\to\infty}$	$2.60(24)\times10^{-3}$	$20(64)\times10^{-5}$	$1.55(58)\times10^{-3}$

system that was most affected by these uncertainties was e^+Sr, which was unbound for some tuning potentials.

VII. MOTIVATION IN TERMS OF THE $(m^{2+}, 2e^-, e^+)$ SYSTEM

The $(m^{2+}, 2e^-, e^+)$ system can be regarded as an analog of the e^+A system where A corresponds to a member of the group II or IIB iso–electronic series [39,40]. In particular, any group II or IIB atoms is described by the $(m^{2+}, 2e^-)$ system with the same ionization potential. It is instructive to look at the stability properties of the $^2P^o$ symmetry of the $(m^{2+}, 2e^-, e^+)$ system.

Table V gives the lowest-energy fragmentation channels for the $(m^{2+}, 2e^-, e^+)$ system as a function of the $X_m=m^{2+}/m_e$ mass ratio. The $L=1$ angular momentum is carried by the relative motion of the different two-body breakup channels.

At the smallest values of X_m, namely, $X_m<0.006\,039$, the lowest energy dissociation channel is that into the $m^{2+}+\text{Ps}^-$ fragments. However, the attractive Coulomb interaction between the two fragments can support an infinite number of electronically stable bound states. Accordingly, one concludes that the $(m^{2+}, 2e^-, e^+)$ system has a $^2P^o$ bound state for $X_m<0.006\,039$.

An estimate of the binding energy of the lowest energy $^2P^o$ state can be deduced by regarding the Ps^- fragment as a negative point charge of mass $3m_e$ [and internal energy equal to $E(\text{Ps}^-)$]. The binding energy of the m^{2+} particle to the Ps^- system in a $1s$ or $2p$ state is given by

$$\varepsilon_{1s}\approx 2\frac{3X_m}{3+X_m};\quad X_m<0.006\,039, \tag{16}$$

TABLE V. The $(m^{2+},2e^-,e^+)$ system dissociation limits and energies for different ranges of the $X_m=m^{2+}/m_e$ mass ratio. These limits and mass ratios do not depend on the total angular momentum of the system.

Dissociation products	Threshold energy	$X_m=m^{2+}/m_e$ mass limits
$(m^{2+},2e^-)+e^+$	$E(m^{2+},2e^-)$	$X_m>0.2907$
$(m^{2+},e^-)+\text{Ps}$	$\frac{-2X_m}{1+X_m}-0.25$	$0.006\,039<X_m<0.2907$
$m^{2+}+\text{Ps}^-$	−0.262 005 07	$X_m<0.006\,039$

$$\varepsilon_{2p}\approx\frac{1}{2}\frac{3X_m}{3+X_m};\quad X_m<0.006\,039. \tag{17}$$

At values of X_m above 0.006 039, the lowest-energy dissociation channel is $(m^{2+},e^-)+\text{Ps}$. The energy of the m^{2+}-Ps^- system relative to the dissociation limit is

$$\varepsilon\approx\frac{1}{2}\frac{3X_m}{3+X_m}+0.012\,005\,07-\frac{2X_m}{1+X_m}. \tag{18}$$

The binding energy given by Eq. (18) is positive for $X_m<0.008$. This critical value of X_m corresponds to a $(m^{2+}, 2e^-)$ ionization energy of about 0.012 hartree. So although there is a range of X_m admitting a stable $^2P^o$ state, the range is too restricted to explain the stability of the e^+Ca $^2P^o$ state.

The $(m^{2+}, 2e^-)$ system, however, is not an exact analog of the calcium atom. The chief difference is that the $4p$ state of Ca^+ is much closer in energy to the Ca^+ $4s$ ground state than the $2p$ state of (m^{2+}, e^-) is to the (m^{2+}, e^-) $1s$ ground state. A crude correction can be made by replacing Eq. (18) with

$$\varepsilon\approx\frac{3}{2}\frac{3X_m}{3+X_m}+0.012\,005\,07-\frac{2X_m}{1+X_m}. \tag{19}$$

The prefactor of 3/2 arises due to the fact that the ratio of the $4s:4p$ energies of Ca^+ is almost 3/4. The binding energy given becomes negative for $X_m>0.024$. The range of binding has been extended, but the ionization energy of the $(m^{2+}, 2e^-)$ system with $X_m=0.024$, namely 0.036 hartree, is still much smaller than that of Ca, 0.225 hartree.

In qualitative terms, this extended range indicates the mechanism for binding. The relatively small energy penalty associated with one of the electrons having nonzero angular momentum means that it does not act to severely inhibit the formation of the Ps^- cluster which is believed to be the structure responsible for binding positrons to divalent atoms with small ionization potentials [39]. It is noted that the $3d$ level of Ca^+ is more tightly bound than the $4p$ level and configurations involving the $3d$ orbital might play some part in binding the positron.

VIII. PERSPECTIVES FOR EXPERIMENTAL DETECTION

The possibilities for experimental verification are best illustrated by reference to the energy-level diagram of e^+Ca and related species shown in Fig. 6. One possible method would be by collision between a Ps beam and neutral calcium. The following reactions involving charge transfers are possible (the binding energy of e^+Ca is taken as 0.019 12 hartree [27])

$$\text{Ps}+\text{Ca}=\text{Ps}+\text{Ca}\ E>0, \tag{20}$$

$$\text{Ps}+\text{Ca}=e^+\text{Ca}(^2S^e)+e^-;\quad E>5.619\ \text{eV}, \tag{21}$$

$$\text{Ps}+\text{Ca}=e^+\text{Ca}(^2P^o)+e^-;\quad E>6.041\ \text{eV}, \tag{22}$$

$$\text{Ps}+\text{Ca}=\text{Ca}^+ +e^-+\text{Ps};\quad E>6.114\ \text{eV}, \tag{23}$$

$$\text{Ps}+\text{Ca}=\text{Ca}^- +e^+;\quad E>6.781\ \text{eV}, \tag{24}$$

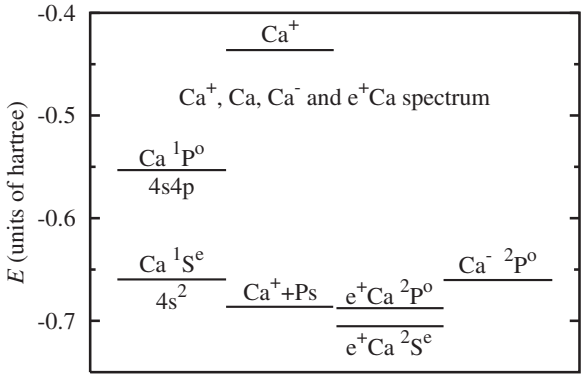

FIG. 6. Energy level diagram showing some of the states of Ca^+, Ca, Ca^-, and e^+Ca. The energy of the Ca^{2+} core is set to zero.

$$\mathrm{Ps} + \mathrm{Ca} = \mathrm{Ca} + e^- + e^-; \quad E > 6.803 \text{ eV}. \tag{25}$$

The key to a successful experiment would be to discriminate between electrons ejected during the formation of positronic calcium and those formed by more mundane reactions. The residual electron left after the formation of positron calcium would have a well-defined energy, while those arising from the ionization of calcium, or fragmentation of Ps would have an energy spread.

Existing technology for positronium beams gives beams with a minimum energy of about 10 eV and an energy spread of about 6 eV full width at half maximum (FWHM) [41]. The existing energy resolution would make the unambiguous detection of the $^2S^e$ state of e^+Ca questionable. Improvements in beam technology would be needed to detect the formation of the $^2S^e$ state. One would look to lower the minimum energy to 5 eV and reduce the energy width of the beam by a factor of 5–10. Other positronic atoms amenable to detection by this method would be those with the larger binding energies, e.g., e^+Mg and e^+Sr [27]. It would be more difficult to detect the $^2P^e$ state with this method since it has an energy threshold that lies within 0.1 eV of the Ca ionization threshold.

The existence of the $^2P^o$ e^+Ca state also means that optical detection of positronic calcium is now a possibility. A dipole transition is allowed between the $^2S^e$ and $^2P^o$ states so detection of a photon with an energy of approximately 0.42 eV (the energy of the e^+Ca ground state relative to the Ca^{2+} core is −0.705 216 hartree [27]) could be used to flag the formation of positronic calcium.

IX. SUMMARY

The present calculations indicate that positronic calcium has a $^2P^o$ excited state with a binding energy of 45 meV. While the present prediction of binding is reliant on an asymptotic analysis to estimate the $J \to \infty$ limit of the orbital basis, the evidence in support of the existence of the excited state is very strong. Indeed, making allowance for ZPE energy corrections gave an estimated binding energy of 71 meV.

The explicit calculation of the $^2P^o$ state of e^+Sr did not give any conclusive evidence of binding. Incorporating a ZPE correction resulted in a bound state with a binding energy of 5.4 meV. However, the uncertainties associated with the ZPE correction mean that no definite conclusion about binding can be made.

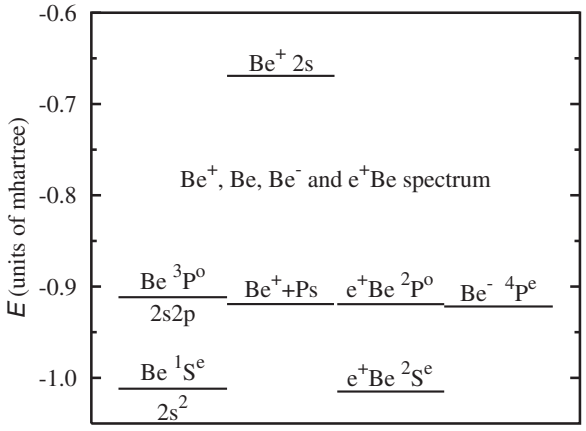

FIG. 7. Energy-level diagram showing some of the states of Be^+, Be, Be^-, and e^+Be. The energy of the Be^{2+} core is at zero.

The binding energy of the $^2P^o$ state of e^+Be is very small, being only 2.6 meV. The position of this state with respect to other states of Be, Be^-, and the Be^++Ps(1s) threshold is shown in Fig. 7. The small binding energy means that the electronic stability of this state is less firmly established than for e^+Ca. However, the small core polarizability of $0.0523a_0^3$ means the wave function is less sensitive to imperfections in the exact definition of the polarization potential. Incorporating the ZPE correction increased the binding energy to an estimated value of 42 meV. It would take only a modest increase in the calculation size (say from 14 LTOs to 16 LTOs per ℓ) to firmly establish the electronic stability of this state.

ACKNOWLEDGMENTS

These calculations were performed on a Linux cluster hosted at the South Australian Partnership for Advanced Computing (SAPAC) and the San Diego State University Computational Sciences Research Center. The authors would like to thank Grant Ward and Dr. James Otto of SAPAC for technical support.

APPENDIX: EVALUATION OF THE HAMILTONIAN

The Hamiltonian can be written most generally as the sum of three one-body operators and three two-body operators:

$$H = T + V = T_1 + T_2 + T_0 + V_{12} + V_{10} + V_{20}. \tag{A1}$$

1. ONE-BODY OPERATORS

The Hamiltonian matrix elements for the one-body operators T_{IJ} can be written

$$\begin{aligned} T_{IJ} &= \langle \phi_a \phi_b [LS]_{\mathcal{A}} \phi_p; L^T S^T | T | \phi_c \phi_d [L'S']_{\mathcal{A}} \phi_q; L^T S^T \rangle \\ &= 2\delta_{p,q}\delta_{L,L'}\delta_{S,S'} N_{ab} N_{cd} [\delta_{b,d}\delta_{\ell_a,\ell_c} \langle \phi_a | T_1 | \phi_c \rangle \\ &\quad + \delta_{a,c}\delta_{\ell_b,\ell_d} \langle \phi_b | T_2 | \phi_d \rangle \end{aligned}$$

$$+(-1)^{\ell_c+\ell_d+L'+S'}\delta_{b,c}\delta_{\ell_a,\ell_d}\langle\phi_a|T_1|\phi_d\rangle$$
$$+(-1)^{\ell_a+\ell_b+L+S}\delta_{a,d}\delta_{\ell_b,\ell_c}\langle\phi_b|T_2|\phi_c\rangle]$$
$$+\delta_{a,c}\delta_{b,d}\delta_{L,L'}\delta_{\ell_p,\ell_q}\langle\phi_p|T_0|\phi_q\rangle. \quad \text{(A2)}$$

The two phase factors, arising from electron antisymmetrization have the same phase due to the fact that $L=L'$ must be true for the scalar one-body operators, T_1 and T_2, to have nonzero matrix elements.

2. THE TWO-BODY OPERATORS

The two-body operators consist of one electron-electron operator and two electron-positron operators. The V_{12} electron-electron matrix element is easily written by treating the positron as a spectator, e.g.,

$$V_{IJ}=\langle\phi_a\phi_b[LS]_{\mathcal{A}}\phi_p;L^TS^T|V_{12}|\phi_c\phi_d[L'S']_{\mathcal{A}}\phi_q;L^TS^T\rangle$$
$$=\delta_{p,q}\delta_{L,L'}\delta_{S,S'}N_{ab}N_{cd}(\langle\phi_a\phi_b[LS]|V_{12}|\phi_c\phi_d[L'S']\rangle$$
$$+(-1)^{\ell_c+\ell_d+L'+S'}\langle\phi_a\phi_b[LS]|V_{12}|\phi_d\phi_c[L'S']\rangle). \quad \text{(A3)}$$

These matrix elements are reduced to using standard techniques, e.g.,

$$\langle\phi_a\phi_b[L]|V_{12}|\phi_c\phi_d[L]\rangle=\sum_k c^k(\ell_a,\ell_b,\ell_c,\ell_d,L)R^k(a,b,c,d), \quad \text{(A4)}$$

where the radial integral is

$$R^k(a,b,c,d)=\int r_1^2dr_1\int r_2^2dr_2\phi_a(r_1)\phi_b(r_2)$$
$$\times\frac{r_<^k}{r_>^{k+1}}\phi_c(r_1)\phi_d(r_2), \quad \text{(A5)}$$

and $r_<=\min(r_1,r_0)$ and $r_>=\max(r_1,r_0)$. The angular factor is

$$c^k(\ell_a,\ell_b,\ell_c,\ell_d,L)=(-1)^{\ell_a+\ell_c+L}\hat{\ell_a}\hat{\ell_b}\hat{\ell_c}\hat{\ell_d}\begin{Bmatrix}l_a & l_b & L\\ l_d & l_c & k\end{Bmatrix}$$
$$\times\begin{pmatrix}\ell_a & k & \ell_c\\ 0 & 0 & 0\end{pmatrix}\begin{pmatrix}\ell_b & k & \ell_d\\ 0 & 0 & 0\end{pmatrix}. \quad \text{(A6)}$$

The electron-electron interaction conserves the intermediate two-electron L and S.

The V_{10} and V_{20} operators have a more complicated structure. The two-electron spin S is conserved (i.e., $S=S'$) but the electron-positron operator can change the two-electron angular momentum. Adopting the notation,

$$\langle\phi_a\phi_b[LS]\phi_p;L^TS^T|V_{10}|\phi_c\phi_d[L'S]\phi_q;L^TS^T\rangle$$
$$=\langle abLp|V_{10}|cdL'q\rangle. \quad \text{(A7)}$$

The matrix element for V_{10} is written

$$\langle V_{10}\rangle=\delta_{bd}N_{ab}N_{cd}\langle abLp|V_{10}|cdL'q\rangle$$
$$+(-1)^{\ell_c+\ell_d+L'+S}\delta_{bc}N_{ab}N_{cd}\langle ab[L]\phi_p|V_{10}|dcL'q\rangle$$
$$+(-1)^{\ell_a+\ell_b+L+S}\delta_{ad}N_{ab}N_{cd}\langle baLp|V_{10}|cdL'q\rangle$$
$$+(-1)^{\ell_a+\ell_b+L+\ell_c+\ell_d+L'}\delta_{ac}N_{ab}N_{cd}\langle baLp|V_{10}|dcL'q\rangle. \quad \text{(A8)}$$

The V_{20} operator gives an expression identical to $\langle V_{10}\rangle$ since the wave function is antisymmetric with respect to electron interchange.

The reduction of the first term of Eq. (A8) is

$$\langle abLp|V_{10}|cdL'q\rangle$$
$$=\sum_k R^k(a,p,c,q)\delta_{bd}$$
$$\times\langle\phi_a\phi_b[LS]\phi_p;L^TS^T\|\mathbf{C}_1^k\cdot\mathbf{C}_0^k\|\phi_c\phi_d[L'S]\phi_q;L^TS^T\rangle, \quad \text{(A9)}$$

where $R^k(a,p,c,q)$ is the radial integral. The angular integral is

$$\langle\phi_a\phi_b[LS]\phi_p;L^TS^T\|\mathbf{C}_1^k\cdot\mathbf{C}_0^k\|\phi_c\phi_d[L'S']\phi_q;L^TS^T\rangle=\delta_{S,S'}\delta_{b,d}(-1)^{\ell_b+\ell_p+\ell_q+L^T}\hat{L}\hat{L'}\hat{\ell_a}\hat{\ell_c}\hat{\ell_p}\hat{\ell_q}\begin{Bmatrix}L & \ell_p & L^T\\ \ell_q & L' & k\end{Bmatrix}\begin{Bmatrix}\ell_a & L & \ell_b\\ L' & \ell_c & k\end{Bmatrix}$$
$$\times\begin{pmatrix}\ell_a & k & \ell_c\\ 0 & 0 & 0\end{pmatrix}\begin{pmatrix}\ell_p & k & \ell_q\\ 0 & 0 & 0\end{pmatrix}. \quad \text{(A10)}$$

Reduction of the other terms of Eq. (A8) is trivial given the reduction of the first term.

[1] J. Mitroy, M. W. J. Bromley, and G. G. Ryzhikh, J. Phys. B **35**, R81 (2002).
[2] D. A. L. Paul and L. Saint-Pierre, Phys. Rev. Lett. **11**, 493 (1963).
[3] V. I. Goldanskii and Y. S. Sayasov, Phys. Lett. **13**, 300 (1964).
[4] V. A. Dzuba, V. V. Flambaum, G. F. Gribakin, and W. A. King, J. Phys. B **29**, 3151 (1996).
[5] K. Iwata, G. F. Gribakin, R. G. Greaves, C. Kurz, and C. M. Surko, Phys. Rev. A **61**, 022719 (2000).
[6] S. J. Gilbert, L. D. Barnes, J. P. Sullivan, and C. M. Surko, Phys. Rev. Lett. **88**, 043201 (2002).
[7] J. Mitroy, Phys. World **15**, 24 (2002).

[8] L. D. Barnes, S. J. Gilbert, and C. M. Surko, Phys. Rev. A **67**, 032706 (2003).
[9] J. P. Marler, L. D. Barnes, S. J. Gilbert, J. P. Sullivan, J. A. Young, and C. M. Surko, Nucl. Instrum. Methods Phys. Res. B **221**, 84 (2004).
[10] M. W. J. Bromley and J. Mitroy, Phys. Rev. Lett. **97**, 183402 (2006).
[11] G. G. Ryzhikh and J. Mitroy, J. Phys. B **31**, 3465 (1998).
[12] M. W. J. Bromley and J. Mitroy, Phys. Rev. A **65**, 012505 (2001).
[13] M. W. J. Bromley and J. Mitroy, Phys. Rev. A **65**, 062505 (2002).
[14] J. Mitroy and M. W. J. Bromley, Phys. Rev. A **73**, 052712 (2006).
[15] J. Mitroy and I. A. Ivanov, Phys. Rev. A **65**, 012509 (2002).
[16] J. Mitroy and M. W. J. Bromley, Phys. Rev. A **67**, 034502 (2003).
[17] J. Mitroy and M. W. J. Bromley, Phys. Rev. A **68**, 052714 (2003).
[18] J. Mitroy and G. G. Ryzhikh, J. Phys. B **32**, 2831 (1999).
[19] V. A. Dzuba, V. V. Flambaum, G. F. Gribakin, and C. Harabati, Phys. Rev. A **60**, 3641 (1999).
[20] C. Schwartz, Phys. Rev. **126**, 1015 (1962).
[21] D. P. Carroll, H. J. Silverstone, and R. P. Metzger, J. Chem. Phys. **71**, 4142 (1979).
[22] R. N. Hill, J. Chem. Phys. **83**, 1173 (1985).
[23] M. W. J. Bromley and J. Mitroy, Int. J. Quantum Chem. **107**, 1150 (2007).
[24] S. Salomonson and P. Oster, Phys. Rev. A **40**, 5559 (1989).
[25] J. Sugar and C. Corliss, J. Phys. Chem. Ref. Data **14**, 1 (1985).
[26] A. Stathopolous and C. Froese Fischer, Comput. Phys. Commun. **79**, 268 (1994).
[27] M. W. J. Bromley and J. Mitroy, Phys. Rev. A **73**, 032507 (2006).
[28] J. R. Rubbmark and S. A. Borgstrom, Phys. Scr. **18**, 196 (1978).
[29] M. W. J. Bromley and J. Mitroy, Nucl. Instrum. Methods Phys. Res. B **247**, 42 (2006).
[30] D. M. Schrader, in *New Directions in Antimatter Physics and Chemistry*, edited by C. M. Surko and F. A. Gianturco (Kluwer Academic Publishers, Dordrecht, The Netherlands, 2001), p. 263.
[31] C. Laughlin, Phys. Lett. **75A**, 199 (1980).
[32] C. F. Fischer and G. Tachiev, At. Data Nucl. Data Tables **87**, 1 (2000).
[33] W. Kutzelnigg and J. D. Morgan III, J. Chem. Phys. **96**, 4484 (1992).
[34] M. W. J. Bromley and J. Mitroy, Phys. Rev. A **66**, 062504 (2002).
[35] V. A. Dzuba, V. V. Flambaum, and C. Harabati, Phys. Rev. A **62**, 042504 (2000).
[36] H. A. Bethe, Phys. Rev. **76**, 38 (1949).
[37] C. Green, U. Fano, and G. Strinati, Phys. Rev. A **19**, 1485 (1979).
[38] M. J. Seaton, Rep. Prog. Phys. **46**, 167 (1983).
[39] J. Mitroy, Phys. Rev. A **66**, 010501(R) (2002).
[40] J. Mitroy and S. A. Novikov, Phys. Rev. A **70**, 032511 (2004).
[41] G. Laricchia, S. Armitage, and D. E. Leslie, Nucl. Instrum. Methods Phys. Res. B **233**, 88 (2005).